

## Enhanced photocatalytic degradation of diazinon by TiO<sub>2</sub>/ZnO/CuO nanocomposite under solar radiation

Mohammad Malakootian<sup>a,c</sup>, Mohammad Mahdi Soori<sup>b,c,\*</sup>

<sup>a</sup>Environmental Health Engineering Research Center, Kerman University of Medical Sciences, Kerman, Iran, email: m.malakootian@yahoo.com (M. Malakootian)

<sup>b</sup>Students Research Committee, School of Public Health, Kerman University of Medical Sciences, Kerman, Iran, Tel. +98 9124651581; email: mhd\_soori@yahoo.com (M.M. Soori)

<sup>c</sup>Department of Environmental Health Engineering, Faculty of Public Health, Kerman University of Medical Sciences, Kerman, Iran

Received 21 March 2021; Received 18 September 2021

---

### ABSTRACT

Diazinon which is one of the most widely used toxins and pesticides, is responsible for contaminating surface and ground water sources all over the world. This study aims to determine the photo-catalytic degradation of diazinon using TiO<sub>2</sub>/ZnO/CuO nanocomposite under solar radiation in aqueous solutions. First, TiO<sub>2</sub>/ZnO nanoparticles were synthesized, then they were doped by 0.5%, 1%, and 2% of copper oxide. To characterize nanoparticles, the scanning electron microscope, energy-dispersive X-ray spectroscopy, X-ray diffraction (XRD), Fourier transform infrared spectroscopy, MAP, and zeta potential analysis were conducted; and also the effects of different variables such as copper dopant percent, pH, nanoparticles dose, initial concentration of diazinon and contact time were evaluated on photo-catalytic reaction using one factor at time procedure. The results showed that the dopant percent of copper oxide was effective for removing diazinon so that doping of 0.5%, 1%, and 2% of copper oxide had the efficiency of 53%, 71%, and 61%, respectively, and they were more than uncoated nanoparticles (TiO<sub>2</sub>/ZnO) in the same condition. Based on the results, the highest removal rate of diazinon after 120 min of reaction time was 91% under optimal conditions (pH = 7, 1% copper dopant, and 2 g/L nanoparticles). Therefore, it can be concluded that the photocatalytic process by TiO<sub>2</sub>/ZnO/CuO nanoparticles could effectively eliminate diazinon under real conditions.

**Keywords:** TiO<sub>2</sub>/ZnO/CuO; photo-catalyst; Diazinon; Thermal nanoparticles synthesis; Aqueous solution

---

### 1. Introduction

Diazinon is an inhaled, digestive, contact, and non-systemic insecticide from the group of organophosphate pesticides. This insecticide is one of the most widely used poisons to control a wide range of agricultural pests [1]. According to World Health Organization (WHO), diazinon is one of the relatively dangerous toxins [2,3] that can enter surface and groundwater sources through the leakage of chemicals, industrial effluent, and

agricultural runoff [4]. WHO guidelines have announced that the maximum allowed amount of diazinon in drinking water is 20 µg/L [5]. On the other hand, United States Environmental Protection Agency (EPA) guidelines have announced that water supplies that contain 20 µg/L of diazinon could be used for 10 d, and others that contain 1 mg/L of diazinon could be used for a lifetime without any health risk. [6,7]. Therefore, due to the low threshold concentration of diazinon, it must remove before reaching the water sources.

---

\* Corresponding author.

Various methods like adsorption, coagulation, biodegradation, etc., are applied to remove various water pollutants [4,8–10]. Because of the presence of non-biodegradable and late-biodegradable compounds in the structure of pesticides and the inadequate efficiency of the mentioned methods for removing toxic compounds, it is necessary to use more efficient methods such as advanced oxidation processes (AOPs) [11–16]. Among the AOPs, the photocatalytic process has high effectiveness in degrading resistant compounds into safe and inert compounds [8]. Different nano-catalysts such as  $\text{TiO}_2$ ,  $\text{Fe}_2\text{O}_3$ ,  $\text{CuO}$ ,  $\text{Fe}_3\text{O}_4$ ,  $\text{SiO}_2$ ,  $\text{WO}_3$ , and rGO are used to perform photocatalytic processes [17–25]. Meanwhile,  $\text{TiO}_2$  is the most commonly used photocatalyst that is applied due to its ease of access, relatively low price, simple laboratory preparation, and high stability [25]. However,  $\text{TiO}_2$  has disadvantages, such as a high band gap (3.2 electron-volts) [26], which leads to low efficiency in visible light and main activity in UV light [25,27]. So, it is necessary to modify  $\text{TiO}_2$  using the compounds that increase the absorption range of the visible light region [25]. Zinc oxide (ZnO) with the direct band-gap of 3.37 eV and exciton binding energy of 60 MW has received vast attention due to high photocatalytic activity, low toxicity, low cost, high corrosion resistance in aqueous solutions [28,29]. The quantum efficiency of ZnO powder is also very high [30,31]. Due to its high energy gap, modification of ZnO's absorption via compounds that could change the absorption from ultraviolet to visible spectrum is necessary [32–35]. The best way to improve light absorption and increase the catalytic activity of  $\text{TiO}_2$  and ZnO in visible light is using low bandgap semiconductors like  $\text{CuO}$  (1.2–1.8 eV), which can absorb a significant portion of visible light and facilitate the transfer of electrons to the high bandgap ( $\text{TiO}_2$ ) semiconductor. Copper oxide ( $\text{CuO}$ ) is also an important semiconductor with a photocatalytic activity that is highly considered due to its unique properties such as non-toxicity, low cost, ease of synthesis, and chemical stability [36,37].

The research aims to determine diazinon degradation from aqueous solution under photocatalytic process unit by  $\text{TiO}_2/\text{ZnO}/\text{CuO}$  nanoparticles and solar radiation.

## 2. Materials and methods

### 2.1. Materials

The chemical reagents including  $\text{CuO}$ ,  $\text{TiO}_2$ ,  $\text{ZnO}$ ,  $\text{NaOH}$ , and  $\text{HCl}$  were all of the analytical grade obtained from Merck Company, Germany. Diazinon to prepare synthetic wastewater was purchased from Sigma Company with a purity of over 98% and used without further purification. The characteristics and molecular structure of diazinon are presented in Table 1.

The stock solution of diazinon was prepared by dissolving 1 g of diazinon in a liter of deionized water, then, samples with the intended concentration made by diluting the stock solution.

### 2.2. Photocatalytic reactor

The reactor used in this study consisted of a 250 mL beaker along with a light source. To conduct the photocatalytic

process, the solar radiation was used as a light source in July from 12:00 to 2:00 pm and the intensity of sunlight in this time was in the range 90,000–85,000 LUX, measured using a LUX meter. Fig. 1 shows a schematic of the reactor used in the study.

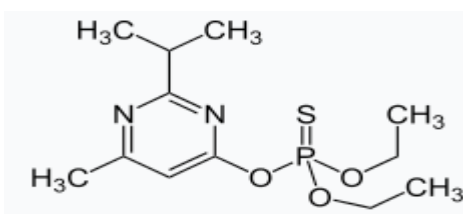
### 2.3. Synthesis of $\text{TiO}_2/\text{ZnO}/\text{CuO}$

$\text{TiO}_2/\text{ZnO}/\text{CuO}$  nanocomposite was synthesized through a one-step hydrothermal process. This is a simple yet practical method for synthesizing nanomaterials. First, 0.05 g of ZnO, 1.5 g of  $\text{TiO}_2$ , and then various values of CuO (0.5, 1, 2 weight percentage of  $\text{TiO}_2+\text{ZnO}$ ) were added to the Teflon liner. Afterward, 10 mL of  $\text{HCl}$  solution was added and, after stirring, the Teflon liner was placed inside the steel reactor at  $120^\circ\text{C}$  for 12 h. Afterward, the liners were emptied and the produced nanoparticles were rinsed with deionized water several times; it was continued until the pH of the nanoparticles was neutralized. Then, the nanoparticles were dried in an oven at  $60^\circ\text{C}$  for 24 h [38]. Fig. 2 shows the used steel autoclave in the synthesis of nanoparticles.

### 2.4. Photocatalytic tests

In this study, various factor such as copper dopant percent (0.5%, 1% and 2%), pH (3, 5, 7, 9 and 11), nanoparticles dose (0, 0.5, 1, 2 and 3 g/L), initial concentration of diazinon (10, 25, 50, 75 and 100 mg/L) at the contact times of 20, 40, 60, 80, 100, and 120 min were investigated on photocatalytic reaction using one factor at time procedure. In the following, the real wastewater including diazinon was tested under optimal conditions obtained in the optimization process. To perform the tests and to measure the concentration of toxin, a VARIAN CP-3800 gas chromatography instrument with FID detector and CP-Sil8-CB column was used. The samples were extracted using liquid chlorobenzene. To determine the photocatalytic process efficiency, the removal percentage of diazinon was calculated by the following equation [39]:

Table 1  
Chemical structure and characteristics of diazinon

Structure	
Chemical formula	$\text{C}_{12}\text{H}_{21}\text{N}_2\text{O}_3\text{PS}$
Molar mass	304.34 g/mol
Boiling point	Decomposes
Solubility in water	40 mg/L
pKa	4.3

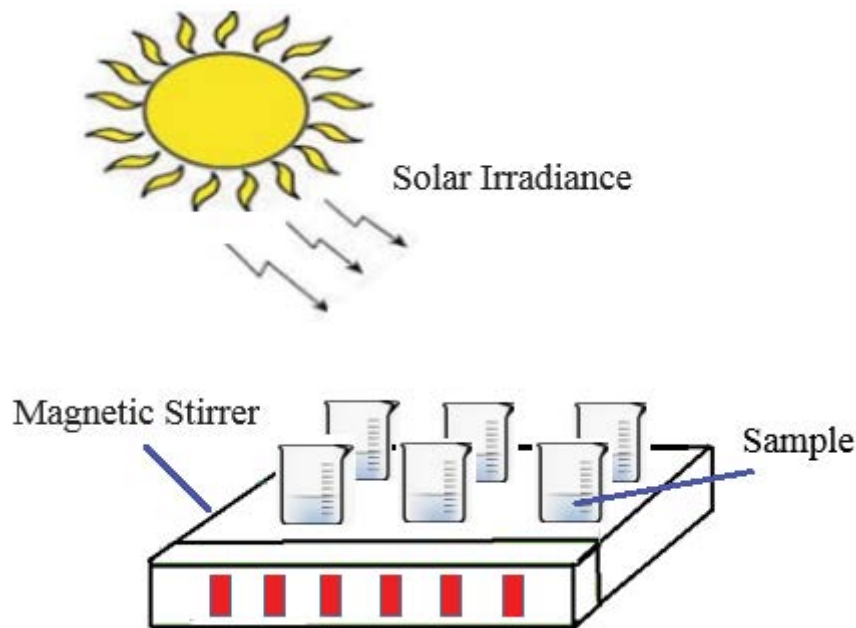


Fig. 1. Schematic representation of the photocatalytic reactor.



Fig. 2. Autoclave used in synthesis of nanoparticles.

$$R = \left[ 1 - \frac{C_f}{C_i} \right] \times 100 \quad (1)$$

where  $R$  is removal efficiency percentage, and  $C_i$  and  $C_f$  are initial concentrations and residual concentrations of diazinon after performing the photocatalytic process (mg/L) respectively.

Before performing photocatalytic activity, in order to do pollutant adsorption and desorption activity by nanoparticles, the samples were kept in the dark for 30 min.

### 2.5. Characterization of nanoparticle

To evaluate the properties and characteristics of the synthesized nanoparticles, various analyses were used. Hence, to describe the shape and size of the nanoparticles, a scanning electron microscope (SEM) image (model: Tscan MIRA3; made in the Czech Republic) was used. In order

to study the crystal structure and order of the nanoparticle crystal lattice, the X-ray spectroscopy (XRD) technic (model: Philips PW-1730; made in the Netherlands) was applied. To study the functional groups of the synthesized nanoparticles, Fourier transform infrared spectroscopy (FTIR) technic (model: Thermo AVATAR; made in the USA) were used, as well as zeta potential of the nanoparticles was measured to evaluate the surface charge and colloidal properties of nanoparticles using the ZEN3600 Malvern made in the United Kingdom.

### 2.6. Determination of $\text{TiO}_2/\text{ZnO}/\text{CuO}$ $\text{pH}_{zpc}$

To obtain  $\text{pH}_{zpc}$  of  $\text{TiO}_2/\text{ZnO}/\text{CuO}$ , about 5 g of NaCl was dissolved in 1,000 mL of distilled water. Then, six flasks were each filled with a 100 ml sample which was taken from the previous solution. The initial pH of these samples was maintained to 2, 4, 6, 8, 10, and 12 by the addition of 0.1 M HCl or 0.1 M NaOH solutions. Next, 0.2 g of the

synthesized  $\text{TiO}_2/\text{ZnO}/\text{CuO}$  was added to each flask and the resultant suspension was shaken at 300 rpm for 48 h. At the end of this experimental series, the final pH of each sample was registered and the  $\text{pH}_{\text{zpc}}$  value shows the intersection point between the initial and final pH curves.

### 3. Results and discussion

#### 3.1. Nanoparticle characterization

Fig. 3 shows SEM images of  $\text{TiO}_2/\text{ZnO}/\text{CuO}$  nanoparticles with 1.5 g of  $\text{TiO}_2$ , 0.05 g of ZnO, and 0.5, 1, and 2 wt.% of CuO with a magnification of 200 nm compared to  $\text{TiO}_2$  and ZnO. SEM results suggested the globular and spherical shape of nanoparticles. In sample A, the particles were in agglomerated form, but in samples B and C, due to the increased amount of CuO, the nanoparticles were fully separated so that any agglomeration wasn't observed and the particles were grains. The effect of doping on  $\text{TiO}_2$  and ZnO led to the grain-coated appearance. In previous studies, a fine-grained coating has been seen on the doped

surface [40]. According to the images, the particles size was in the range of 20–130 nm.

To evaluate the presence of elements and their weight percentages in synthesized nanoparticles, energy-dispersive X-ray spectroscopy (EDX) technique was used. In Fig. 4, the EDX spectrum of  $\text{TiO}_2/\text{ZnO}/\text{CuO}$  (0.5%, 1% and 2%) nanoparticles are shown. In this spectrum, X-axis shows the measured energy and Y-axis shows the number of times that particular energy is detected. According to the appearance of the peaks, the ratio between the intensities (peak height of elements) expresses the ratio between concentrations. The higher peaks in the spectrum also mean a higher concentration of the desired elements in the sample. The results showed that the elements of  $\text{TiO}_2/\text{ZnO}/\text{CuO}$  (1%) nanoparticles were O, Ti, Cu, and Zn by weight percentages of 36.01, 61.40, 1.13, and 1.46 respectively. Accordingly, the synthesis and dopant process was properly done and the nanoparticle had no impurities [41].

High-resolution scanning transmission electron microscopy (HR-STEM) is another important technique that

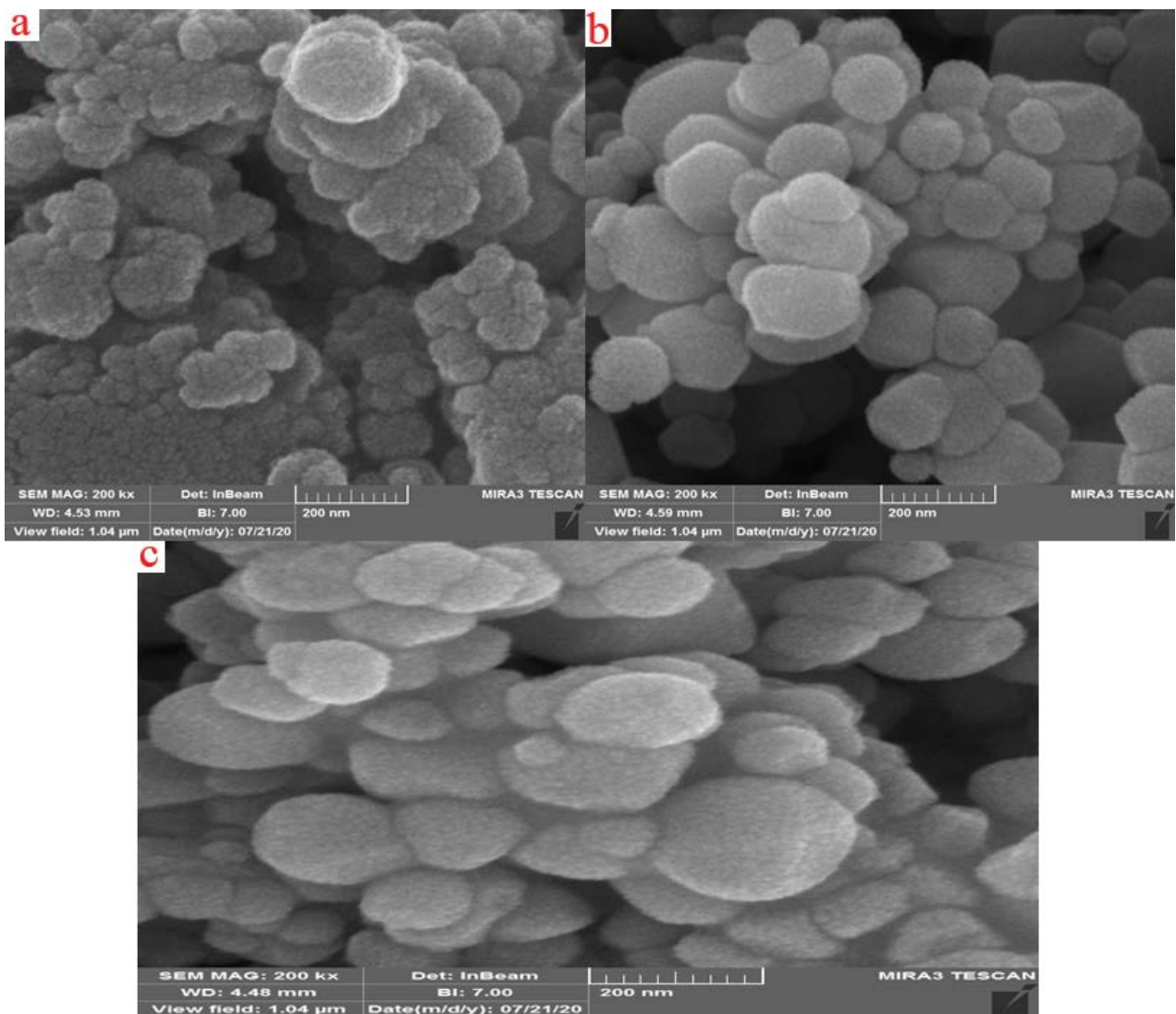


Fig. 3. SEM images of nanoparticles (a)  $\text{TiO}_2@\text{ZnO}@\text{CuO}$  (0.5%), (b)  $\text{TiO}_2@\text{ZnO}@\text{CuO}$  (1%), and (c)  $\text{TiO}_2@\text{ZnO}@\text{CuO}$  (2%).

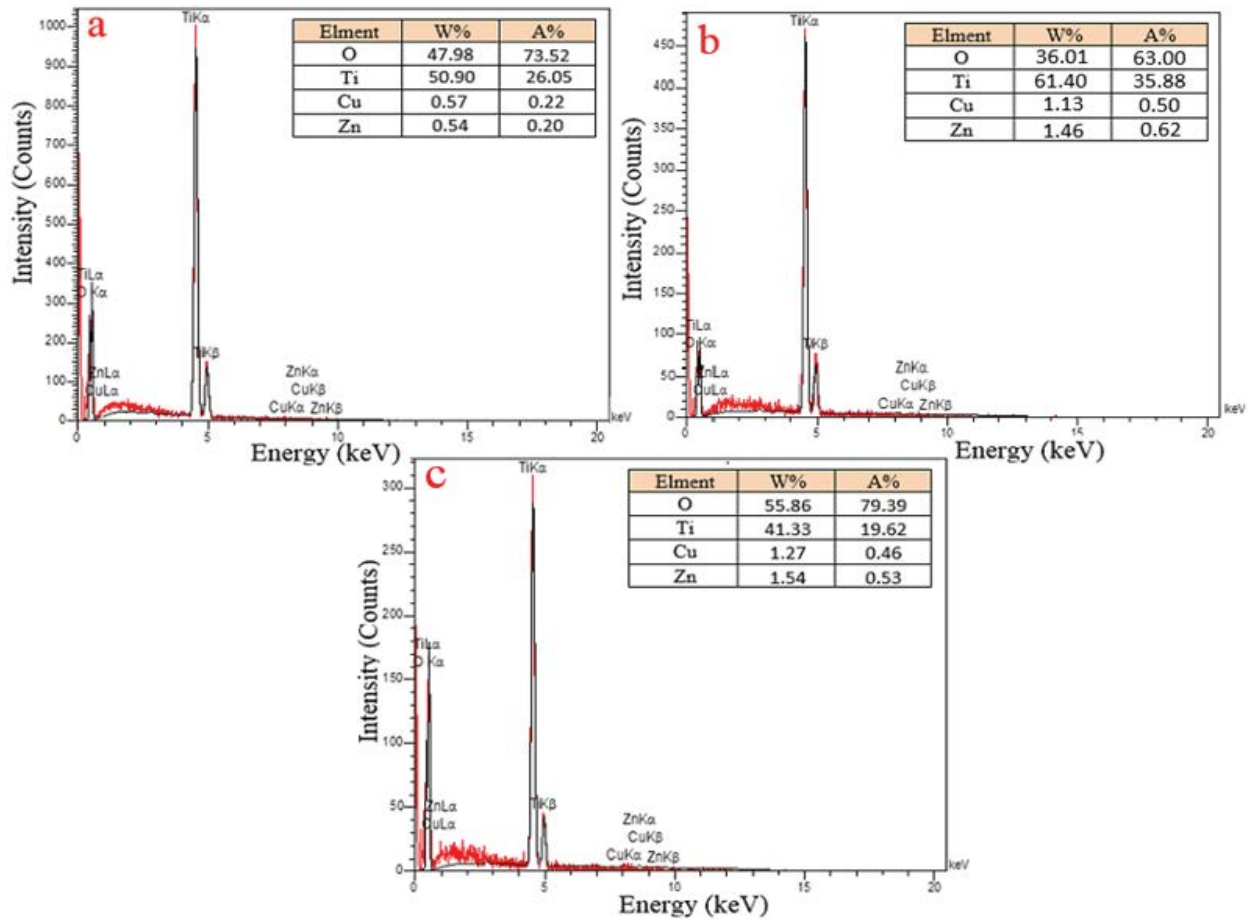


Fig. 4. Energy-dispersive X-ray spectroscopy of nanoparticles (a) TiO<sub>2</sub>@ZnO@CuO (0.5%), (b) TiO<sub>2</sub>@ZnO@CuO (1%), and (c) TiO<sub>2</sub>@ZnO@CuO (2%).

allows for direct imaging of the atomic structure of the material, in fact, it is powerful instrumentation to study properties of materials on the atomic scale, such as semiconductors, metals [54]. HR-STEM mapping can provide vital information about nanoparticles. In MAP analysis, elements in an image can be presented based on their frequently distribution. Fig. 5 shows the mapping images of O, Cu, Zn, and Ti and combines the elements of TiO<sub>2</sub>, ZnO, CuO (1%) nanoparticles. The elemental frequency image showed that these elements were properly distributed in the particles and any impurities weren't observed. The frequency of the elements was fully consistent with the synthesized values. The synthesized nanoparticles contained O, Cu, Zn, and Ti elements. On the other hand, the results of this analysis were complementary to the EDX technique.

XRD is a tool to study the atomic and molecular structure of a crystal by creating a crystallographer of material. In other words, it is provided information on the determination of phases and structure of crystalline nanoparticles. XRD spectrum of TiO<sub>2</sub>-ZnO-CuO (0.5%, 1% and 2%) is shown in Fig. 6. Given that 1.5 g for TiO<sub>2</sub> is the maximum value in the synthesis of nanoparticles, the results of index peaks at  $2\theta = 25.6^\circ$ ,  $38.1^\circ$ , and  $63^\circ$  following JCPDS No: 21-1272 standard, were in agreement with the presence of anatase phase, TiO<sub>2</sub>, in the nanocomposite structure

[42]. On the other hand, the peak at  $2\theta = 47.8^\circ$  and  $54.5^\circ$  are related to the presence of Zn, and the corresponding peak of CuO was at  $2\theta = 68.8^\circ$ ,  $70.9^\circ$  and  $76.6^\circ$ . All TiO<sub>2</sub> peaks were also appeared after adding ZnO and CuO as dopants; therefore, it did not effect on the crystal structure of TiO<sub>2</sub> nanoparticles [43]. In the XRD pattern (Fig. 6b) by adding Zn and Cu dopant, the anatase phase was affected in a way that the height of peaks became taller and wider. The XRD pattern determined that the intensity of peaks and a partial displacement of peaks could occur when doping process has increased [44].

Fourier-transform infrared spectroscopy is a technique used to get an infrared spectrum of absorption or emission of a solid and corresponding of exiting the functional group. So, by applying FR-IR technic, the functional groups of nanoparticles will be identified. The results of FT-IR of TiO<sub>2</sub>/ZnO/CuO (0.5%, 1%, and 2%) nanoparticles are shown in Fig. 7. Based on the FT-IR plot, several weak peaks were in  $3,400\text{ cm}^{-1}$  and  $2,900\text{ cm}^{-1}$  regions in TiO<sub>2</sub> that were related to vibration tensile bond of O-H and another vibration in the region of  $16,30\text{ cm}^{-1}$  related to flexural vibration bond of water molecules. In the determined absorption spectrum for TiO<sub>2</sub> nanoparticles, the highest peaks were in the  $680\text{ cm}^{-1}$  regions which corresponded to the flexural vibration bond of Ti-O.

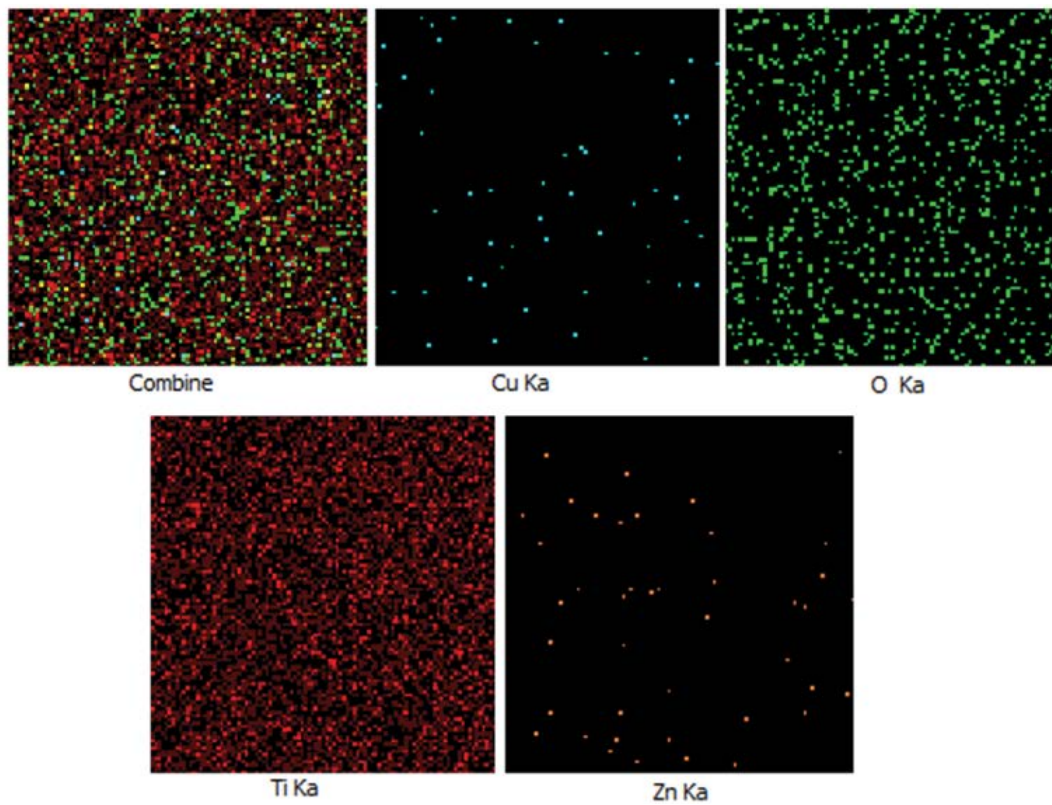


Fig. 5. High-resolution scanning transmission electron microscopy (HR-STEM) elemental mapping images  $\text{TiO}_2@ZnO@CuO$  (1%).

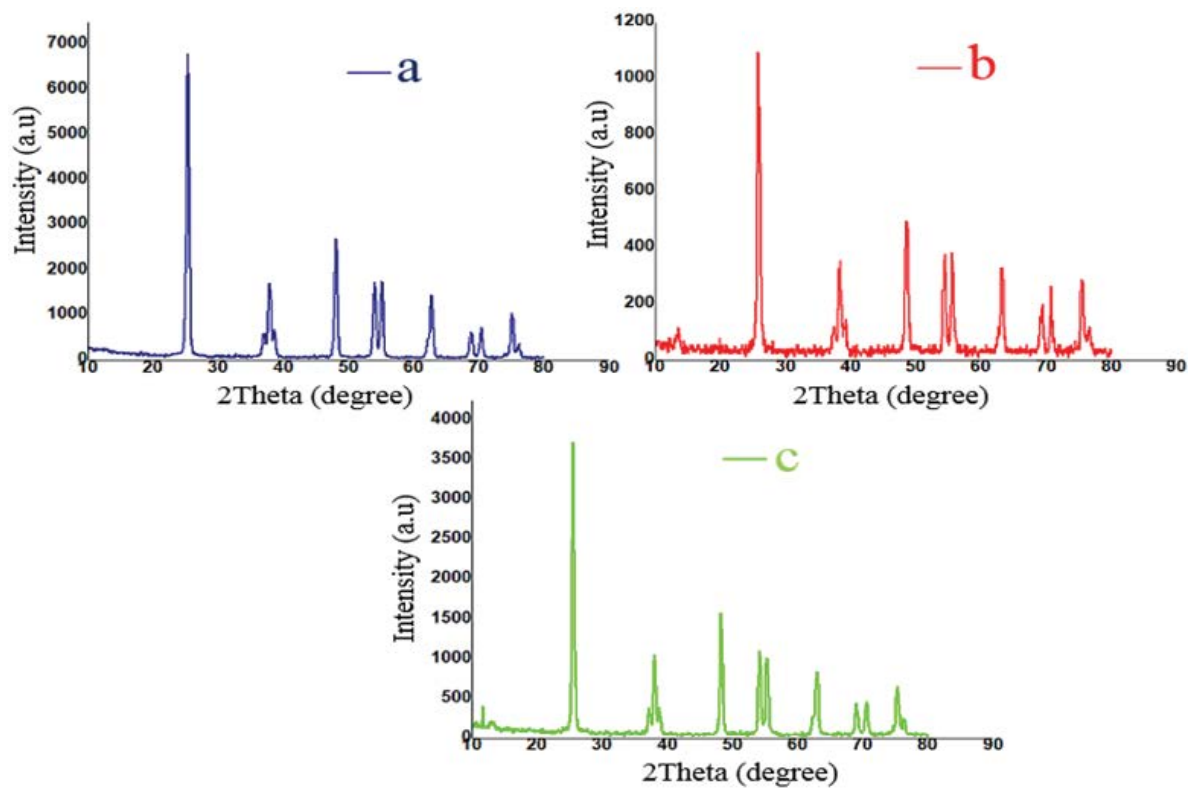


Fig. 6. The X-ray diffraction spectrum of produced nanoparticles (a)  $\text{TiO}_2@ZnO@CuO$  (0.5%), (b)  $\text{TiO}_2@ZnO@CuO$  (1%), and (c)  $\text{TiO}_2@ZnO@CuO$  (2%).

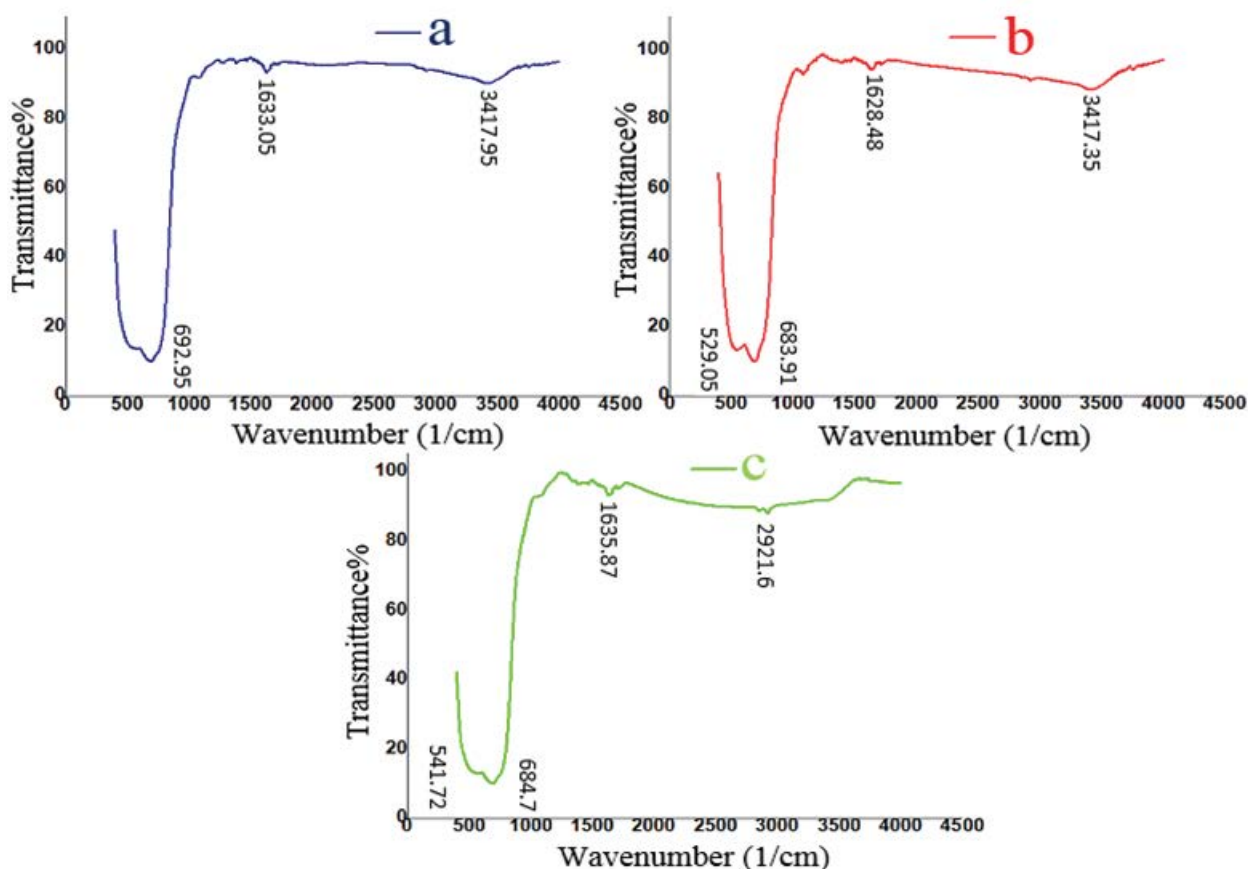


Fig. 7. Fourier transform infrared spectroscopy of nanoparticles (a)  $\text{TiO}_2/\text{ZnO}/\text{CuO}$  (0.5%), (b)  $\text{TiO}_2/\text{ZnO}/\text{CuO}$  (1%), and (c)  $\text{TiO}_2/\text{ZnO}/\text{CuO}$  (2%).

Zeta potential is important for examining the colloidal suspension properties. Zeta electrical potential of  $\text{TiO}_2/\text{ZnO}/\text{CuO}$  (0.5%, 1%, and 2%) was measured at the optimal pH (Fig. 8). Hence, the suspension of 0.01 g of nanoparticles was prepared in 5 ml of distilled water and, before measuring the zeta potential, all the samples were exposed to ultrasonic waves for 15 min to disperse particles in the samples. The results of zeta potential (Table 2) showed that along with the doped nanoparticles, the zeta potential and motion increased so that the zeta potential in the nanoparticles with CuO (0.5, 1, and 2) were  $-28.7$ ,  $-28.9$ , and  $-40.8$  mV, respectively. It is clear that doping increased the surface area and surface charge of  $\text{TiO}_2/\text{ZnO}$  nanoparticles.

### 3.2. Effect of factor on photocatalytic activity

#### 3.2.1. Effect of dopant percent

In order to determine the effect of CuO percent on the photocatalytic activity potential of  $\text{TiO}_2/\text{ZnO}$  composite to degrade of diazinon, the value of CuO (0.5%, 1%, and 2%) were investigated with the following conditions. The photocatalytic removal efficiency of diazinon with doped  $\text{TiO}_2/\text{ZnO}$  nanoparticles and  $\text{TiO}_2/\text{ZnO}$  with 0.5%, 1%, and 2% of copper oxide for 120 min were equal to 50%, 53%, 71%, and 61% (Fig. 9). It is clear that the dopant percent can affect the process so that 1% dopant had better efficiency than 0.5%

and 2%. This could be due to the reduced energy gap of nanoparticles, its higher activity than light, and increased photocatalytic activity of doped nanoparticles. In the study conducted by Zandsalimi et al. [45] entitled "Examining photocatalytic removal 2–4-dichlorophenoxy from aqueous solutions with tungsten metal oxide-doped zinc oxide nanoparticles immobilized on glass beads" were found that the nanoparticle doping percent can impact the process, so that 1% dopant had better efficiency than 0.5% and 2%. In another study conducted by Abdollahi et al. [46], they performed a study on the characteristics of manganese-doped zinc oxide nanoparticles, they synthesized 0.5%, 1%, 1.5%, and 2% of manganese as dopant with ZnO and the results showed that manganese concentration of 1% had finer particle sizes, so that 77% of the particles had the size between 15 and 35 nm. At this percentage, the particles were fully isolated and no adhesion was observed between the particles. So, as can be seen from Fig. 9, coating of copper oxide on the  $\text{TiO}_2/\text{ZnO}$  nanoparticles has improved its photocatalytic activity for degradation of diazinon, and the best percentage of copper oxide for the doping process was 1%.

#### 3.2.2. Effect of pH

One of the most effective parameters affecting chemical processes such as photocatalytic is pH, which can change

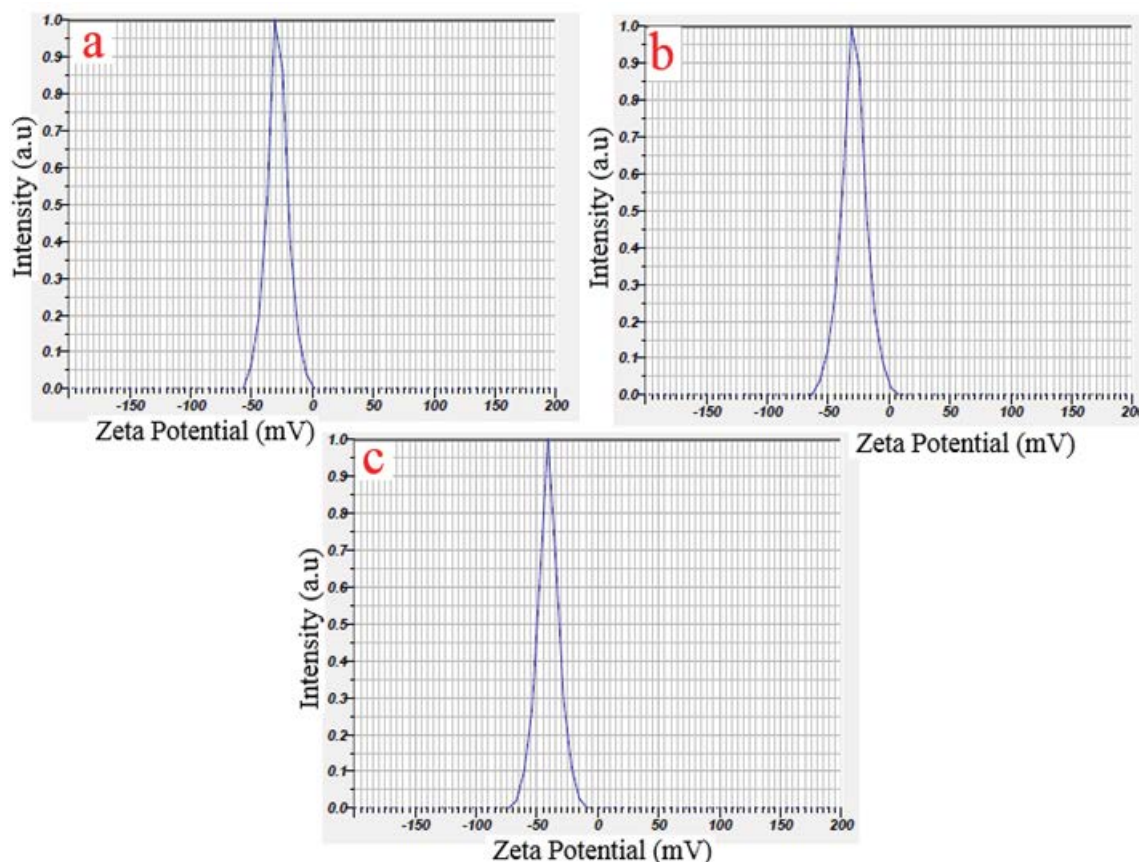


Fig. 8. Zeta potential of (a)  $\text{TiO}_2\text{@ZnO@CuO}$  (0.5%), (b)  $\text{TiO}_2\text{@ZnO@CuO}$  (1%), and (c)  $\text{TiO}_2\text{@ZnO@CuO}$  (2%).

Table 2

Effective diameter and zeta potential (PALS method) details of bare and doped  $\text{TiO}_2$  NPs using the Smoluchowski model

Nanoparticles	Zeta potential (mV)	Mobility ( $\text{cm}^2/\text{Vs}$ )
$\text{TiO}_2\text{:ZnO-CuO}$ (0.5%)	-28.7	-0.000223
$\text{TiO}_2\text{:ZnO-CuO}$ (1%)	-28.9	-0.000224
$\text{TiO}_2\text{:ZnO-CuO}$ (2%)	-40.8	-0.000314

the surface charge of molecules and materials. Producing values of active free radicals such as hydroxyl radicals in the photocatalytic process are highly affected by the pH of the solution [47]. Before conducting the photocatalytic tests, the analysis of  $\text{pH}_{\text{pzc}}$  showed that the  $\text{pH}_{\text{pzc}}$  of the  $\text{TiO}_2/\text{ZnO}/\text{CuO}$  nanoparticle was about 7. So, under this condition, the main functional groups of  $\text{TiO}_2/\text{ZnO}/\text{CuO}$  can be negative charges by  $\text{H}^+$  protons at  $\text{pH} < \text{pH}_{\text{pzc}}$ . On the other hand, the surface of  $\text{TiO}_2/\text{ZnO}/\text{CuO}$  nano-composite at  $\text{pH} > 7$ , will be saturated by negative charges of  $\text{OH}^-$  ions.

Also,  $\text{pK}_a$  of diazinon was about 8.7 in which different diazinon species are available in the solution, based on the pH value above or below 7. So, the diazinon molecules at  $\text{pH} = 7$ ,  $\text{pH} > 7$ , and  $\text{pH} < 7$  can be in the forms of zwitterion, anionic, and cationic, respectively.

The results of the effect of pH on the photocatalytic removal of diazinon are presented in Fig. 10. It showed that

the removal percentage in 120 min in pH of 3, 5, 7, 9, and 11 was equal to 62%, 63%, 87%, 62%, and 61%, respectively. The high efficiency in neutral pH can be due to the maximum production of hydroxyl radicals and  $\text{h}^+$  (hole<sup>+</sup>) under such circumstances. Thus, to attack organic compounds by these radicals with strong oxidation potential and contacting of pH was much faster [48], also it is because the surface charges of  $\text{TiO}_2/\text{ZnO}/\text{CuO}$  nano-composite are being negative and simultaneously the diazinon molecules are in protons forms in the solution. Hence, negative sites on the nano-catalyst surface can be effective in absorbing diazinon, and the increased pH level would be associated with the increasing degrading capability of diazinon [49].

In the study conducted by Leng et al. [50], increasing the pH of the dyed solution from 6.5 to 11 significantly increased the dye removal and, at the pH above 11, the efficiency removal was rapidly increasing. In another study conducted by Houas et al. [51], it was reported that for 50% degradation of methylene blue with the constant concentration of 40 mM, the removal of methylene blue was faster at alkaline pHs.

### 3.2.3. Effect of nanoparticles dose

By considering the costs as a limiting economic factor, the amount of nanoparticles used in the process is one of the most important issues in photocatalytic technology. The results of the study on the effect of  $\text{TiO}_2/\text{ZnO}/\text{CuO}$



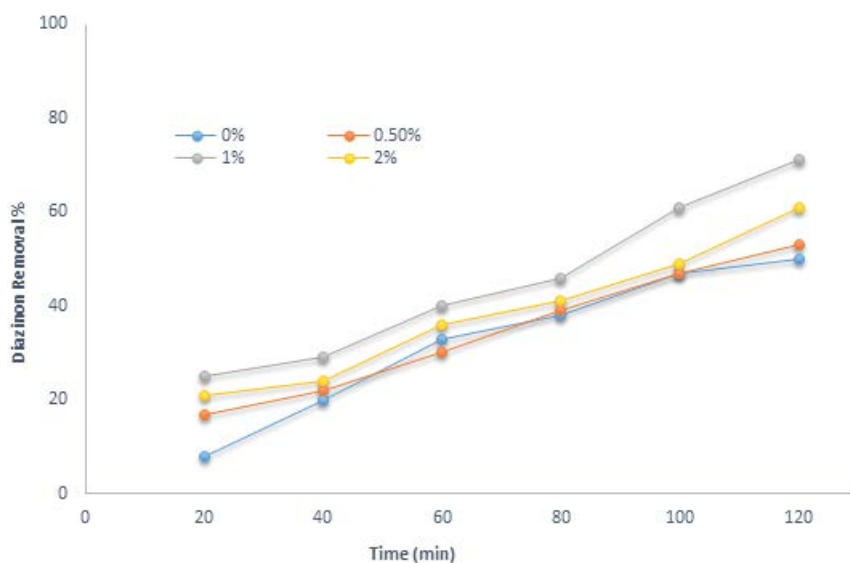


Fig. 9. Effect of copper oxide percentage on removal percentage (initial diazinon concentration = 50 mg/L; pH = 7; dosage of nanoparticle suspension 1.5 g/L).

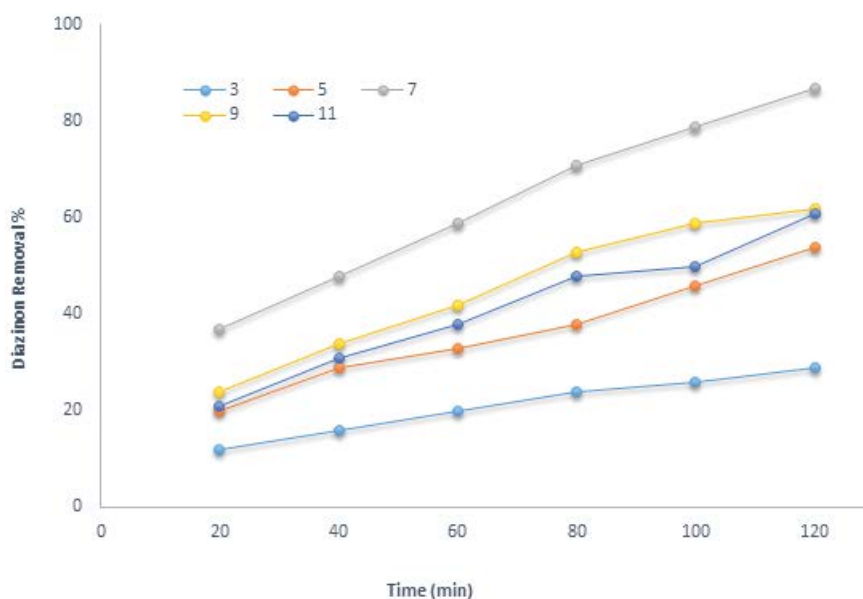


Fig. 10. Effect of pH on removal percentage (initial concentration = 50 mg/L;  $\text{TiO}_2\text{@ZnO@CuO}$  (1%); nanoparticle dose 1.5 g/L).

(1%) nanoparticle dose in the photocatalytic degradation of diazinon are shown in Fig. 11. The result indicates that by increasing the number of nanoparticles, the removal efficiency of the diazinon improved in that way the removal percentage for 0.1, 0.5, 1, 2, and 3 mg/L of the nanoparticles at 120 min was equal to 18%, 40%, 58%, 85%, and 56% respectively. It can justify that by increasing the amount of catalyst, the available active site of the catalyst increase. Thus, it led to an increase in the production of hydroxyl radicals and other oxidizing radicals as well as positive holes ( $h^+$ ) [52]. Moreover, the earlier studies have shown that increasing the number of nanoparticles is directly related to increasing filtration efficiency to a certain extent and has no impact if exceeding a specified level. However,

it could reduce efficiency by disrupting the path of light in suspended particles [53]. Another important point is that when the doping process is carried out, it prevents the recombination of electrons and holes, which leads to increase photocatalytic efficiency. The results of the study conducted by Chakrabarti and Dutta [55]; showed that, with increasing the amount of ZnO catalyst, the photocatalytic degradation was also increased, which was due to increased activity levels on the catalyst and, consequently, increased production of hydroxyl and superoxide radicals [54]. On the other hand, increasing the dose of catalyst beyond the optimal value reduced the degradation rate, which was mainly due to increase turbidity in the passages of light into the solution. In the study conducted by

Naghan et al. [56] which examined the effective parameters for the photocatalytic degradation of phenol in the presence of ZnO under UVC light, the results showed that the efficiency was obtained about 94.24% under optimal conditions of catalyst dose of 15 g/L, initial phenol concentration of 10 mg/L, contact time of 30 min, and pH of 5. The results demonstrated that by increasing the catalyst dose to 0.3 g, the process efficiency was reduced to 75%.

#### 3.2.4. Effect of initial concentration

The initial concentration of diazinon is another factor which considers as one of the effective parameters on

photocatalytic degradation. The results of the effect of initial concentration on the photocatalytic process are presented in Fig. 12. According to the result, an increase in the concentration of diazinon led to reducing the removal efficiency so that the removal percentage in concentrations of 10, 25, and 50 mg/L were 94%, 85%, 77%, 59%, and 53%, respectively. This may be due to the point that, by increasing the initial concentration of diazinon, the higher number of catalyst surface active sites was covered, which reduced the production of oxidizing radicals and, finally, led to a decrease rate of degradation [57]. Reduction of diazinon degradation by increasing the concentration of diazinon was the result of reduced light penetration or lower active sites on the catalyst

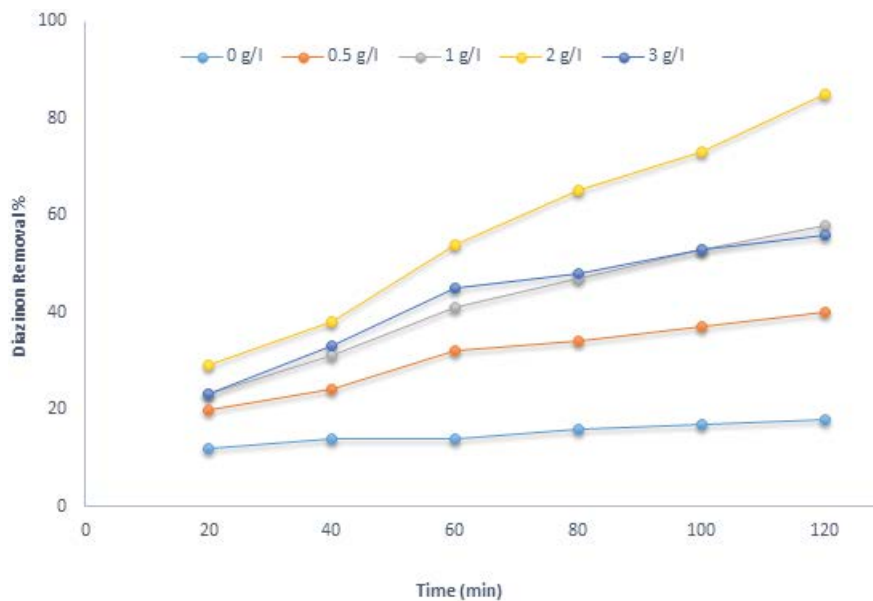


Fig. 11. Effect of nanoparticle dosage on removal percentage (initial concentration = 50 mg/L; pH = 7;  $\text{TiO}_2\text{:ZnO@CuO}$  (1%); nanoparticle dose 1.5 g/L).

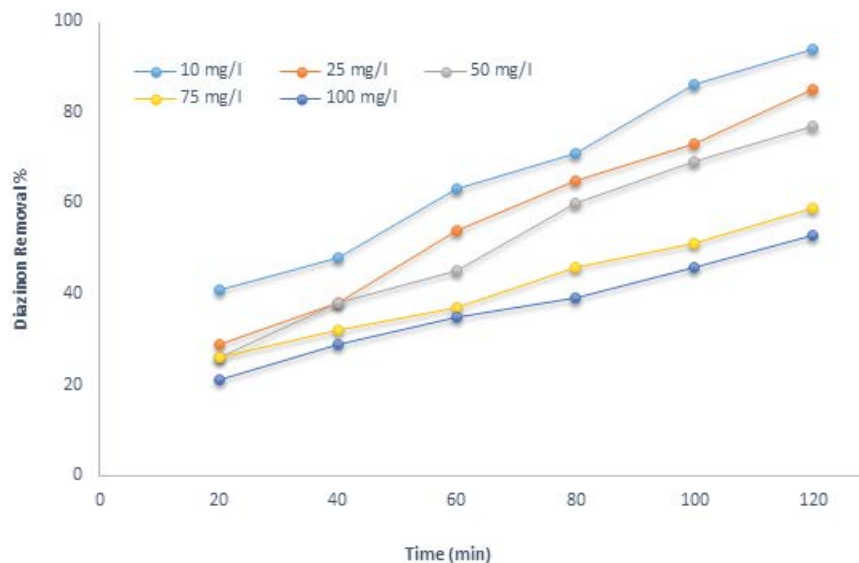


Fig. 12. Effect of diazinon concentration on removal percentage (pH = 7;  $\text{TiO}_2\text{:ZnO-CuO}$  (1%); dosage of nanoparticle suspension 2 g/L).

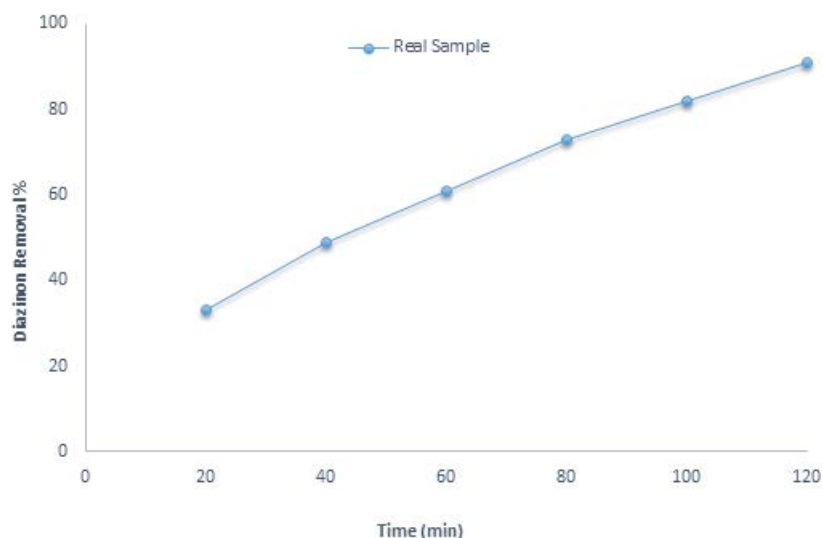


Fig. 13. Effect of photocatalytic process on real sample (pH = 7;  $\text{TiO}_2/\text{ZnO}/\text{CuO}$  (1%); dosage of nanoparticle suspension 2 g/L).

to absorb UV light for production of hydroxyl radicals. Thus, by increasing the concentration of diazinon, most of the diazinon molecules were adsorbed on the surface of the nanoparticles and prevented the production of hydroxyl radicals. Therefore, the efficiency of the process was reduced. Other studies have reached similar conclusions [58–61].

### 3.2.5. Effect of contact time

Contact time is an important parameter in the removal of diazinon under photocatalytic degradation. The results of the effect of contact time on the photocatalytic degradation of diazinon showed that increasing contact time, led to enhance the removal efficiency of diazinon. Regarding this situation, it is obvious that the production of free hydroxyl radicals in the conductive band increased by increasing contact time [62]. Moreover, by increasing contact time, the removal efficiency was raised due to the more opportunity of nanoparticles for generating free hydroxyl radicals and photocatalytic reactions. In fact, by increasing contact time, the exposure to light increases, and more oxidation reactions occur in the presence of hydroxyl radicals [63]. In the study conducted by Alalm et al. [64], entitled “Photocatalytic degradation of phenol by  $\text{TiO}_2/\text{AC}$ ”, the results showed that under optimal conditions, using  $\text{TiO}_2$ , 53% and 80% of phenol were degraded after 30 and 150 min of radiation, respectively, and using  $\text{TiO}_2/\text{AC}$ , 40% and 100% of phenol were degraded after 15 and 120 min of radiation, respectively.

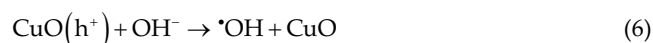
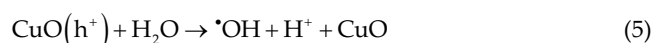
### 3.2.6. Photocatalytic degradation of real diazinon under obtained optimal condition

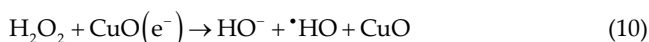
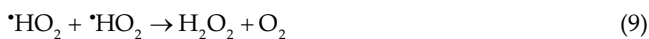
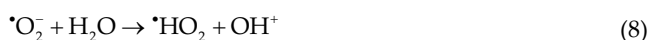
To evaluate the photocatalytic degradation of diazinon in real conditions, the real sample was taken from a diazinon manufacturing factory including 25 mg/L of diazinon concentration and it was exposed to solar radiation under optimal conditions. The achieved results are shown in Fig. 13. Based on the result, it was found that the removal efficiency of 91% was obtained after 120 min reaction time.

It is cleared that the photocatalytic process by  $\text{TiO}_2/\text{ZnO}/\text{CuO}$  nanoparticle had good efficiency in removing diazinon under optimal conditions.

### 3.2.7. Photocatalytic degradation mechanism

One of the main factors needed for photocatalytic reactions is semiconductor materials such as CuO. The main characteristic of the material is having conduction and gap bands in its structure which can lead to a transfer of an electron from the gap band to the conduction band by getting the photon energy and creating cavities (holes<sup>+</sup>, h<sup>+</sup>) at the surface of the catalyst simultaneously [Eqs. (2)–(4)]. The formed h<sup>+</sup> can directly decompose diazinon or their reaction with water molecules product of radical  $\cdot\text{OH}$  and the generated radicals eliminate organic matter [Eqs. (5)–(6)]. On the other side, abandoned electrons can react with the oxygen and they generate  $\cdot\text{O}_2^-$  radical [Eqs. (7)–(8)]. The  $\cdot\text{O}_2^-$  radicals, first generate radical  $\cdot\text{HO}_2$  and then hydrogen peroxide by reacting with water molecules. Moreover, hydrogen peroxide can generate radical  $\cdot\text{OH}$  by getting an electron [Eqs. (9)–(10)]. The generated oxidizing or reducing agent can attack diazinon and it decomposes into water and carbon dioxide as well as a by-product.





#### 4. Conclusion

In this study, the photocatalytic degradation of the diazinon was investigated using CuO-doped TiO<sub>2</sub>/ZnO nanoparticles and before them, the characterization analyses of TiO<sub>2</sub>/ZnO/CuO nanoparticles were conducted by SEM, EDX, FTIR, XRD, MAP, and zeta potential. The results showed that the addition and doping of copper to TiO<sub>2</sub> and ZnO nanoparticles increased the photocatalytic activity of nanoparticles and ease of its activating by visible light. The suitable dopant percent in this process was 1% and had higher efficiency than 0.5% and 2%. The neutral pH had the highest removal efficiency of diazinon. Also, by increasing catalyst dose and contact time, the removal efficiency increased, while increasing the initial concentration of diazinon led to reducing the efficiency. According to the result, it can be concluded that the photocatalytic process by TiO<sub>2</sub>/ZnO/CuO nanoparticles could effectively eliminate diazinon under real conditions.

#### Acknowledgments

This paper was derived from the research project approved by Student Research Committee, Kerman University of Medical Sciences, under no. 98001123, which was funded by Vice Presidency for Research and Technology of this university.

#### References

- [1] A. Toolabi, M. Malakootian, M.T. Ghaneian, A. Esrafil, M.H. Ehrampoush, M. Askar Shahi, M. Tabatabaei, M. Khatami, Optimizing the photocatalytic process of removing diazinon pesticide from aqueous solutions and effluent toxicity assessment via a response surface methodology approach, *Rend. Lincei Sci. Fis. Nat.*, 30 (2019) 155–165.
- [2] E. Fatahi, S. Joursaraei, K. Parivar, A. Moghadamnia, Influence of diazinon on spermatogenesis in mice, *Koomesh J. Semnan Univ. Med. Sci.*, 25 (2007) 75–81.
- [3] N. Daneshvar, S. Aber, M.S. Dorraji, A. Khataee, M.H. Rasoulifard, Photocatalytic degradation of the insecticide diazinon in the presence of prepared nanocrystalline ZnO powders under irradiation of UV-C light, *Sep. Purif. Technol.*, 58 (2007) 91–98.
- [4] A. Jonidi-Jafari, M. Shirzad-Siboni, J.-K. Yang, M. Naimi-Joubani, M. Farrokhi, Photocatalytic degradation of diazinon with illuminated ZnO-TiO<sub>2</sub> composite, *J. Taiwan Inst. Chem. Eng.*, 50 (2015) 100–107.
- [5] G. Moussavi, H. Hossaini, S.J. Jafari, M. Farokhi, Comparing the efficacy of UVC, UVC/ZnO and VUV processes for oxidation of organophosphate pesticides in water, *J. Photochem. Photobiol., A*, 290 (2014) 86–93.
- [6] L. Ferencz, A. Balog, A pesticide survey in soil, water and foodstuffs from central Romania, Carpathian J. Earth Environ. Sci., 5 (2010) 111–118.
- [7] L. Pogačnik, M. Franko, Determination of organophosphate and carbamate pesticides in spiked samples of tap water and fruit juices by a biosensor with photothermal detection, *Biosens. Bioelectron.*, 14 (1999) 569–578.
- [8] M.N. Chong, B. Jin, C.W. Chow, C. Saint, Recent developments in photocatalytic water treatment technology: a review, *Water Res.*, 44 (2010) 2997–3027.
- [9] F. Akbari, M. Khodadadi, A. Hossein Panahi, A. Naghizadeh, Synthesis and characteristics of a novel FeNi<sub>3</sub>/SiO<sub>2</sub>/TiO<sub>2</sub> magnetic nanocomposites and its application in adsorption of humic acid from simulated wastewater: study of isotherms and kinetics, *Environ. Sci. Pollut. Res.*, 26 (2019) 32385–32396.
- [10] M. Khodadadi, T.J. Al-Musawi, M. Kamranifar, M.H. Saghi, A. Hossein Panahi, A comparative study of using barberry stem powder and ash as adsorbents for adsorption of humic acid, *Environ. Sci. Pollut. Res.*, 26 (2019) 26159–26169.
- [11] M. Shirzad Siboni, M. Samadi, J. Yang, S.M. Lee, Photocatalytic reduction of Cr(VI) and Ni(II) in aqueous solution by synthesized nanoparticle ZnO under ultraviolet light irradiation: a kinetic study, *Environ. Technol.*, 32 (2011) 1573–1579.
- [12] M. Shirzad Siboni, M.-T. Samadi, J.-K. Yang, S.-M. Lee, Photocatalytic removal of Cr(VI) and Ni(II) by UV/TiO<sub>2</sub>: kinetic study, *Desal. Water Treat.*, 40 (2012) 77–83.
- [13] R. Andreozzi, V. Caprio, A. Insola, R. Marotta, Advanced oxidation processes (AOP) for water purification and recovery, *Catal. Today*, 53 (1999) 51–59.
- [14] A. Hossein Panahi, A. Meshkinian, S.D. Ashrafi, M. Khan, A. Naghizadeh, G. Abi, H. Kamani, Survey of sono-activated persulfate process for treatment of real dairy wastewater, *Int. J. Environ. Sci. Technol. (Tehran)*, 17 (2020) 93–98.
- [15] T.J. Al-Musawi, H. Kamani, E. Bazrafshan, A. Hossein Panahi, M.F. Silva, G. Abi, Optimization the effects of physicochemical parameters on the degradation of cephalixin in sono-Fenton reactor by using Box-Behnken response surface methodology, *Catal. Lett.*, 149 (2019) 1186–1196.
- [16] B. Barikbin, F.S. Arghavan, A. Othmani, A. Hossein Panahi, N. Nasseh, Degradation of tetracycline in Fenton and heterogeneous Fenton like processes by using FeNi<sub>3</sub> and FeNi<sub>3</sub>/SiO<sub>2</sub> catalysts, *Desal. Water Treat.*, 200 (2020) 262–274.
- [17] N. Rādhika, R. Selvin, R. Kakkar, A. Umar, Recent advances in nano-photocatalysts for organic synthesis, *Arabian J. Chem.*, 12 (2019) 4550–4578.
- [18] S. Dehghan, A.J. Jafari, M. FarzadKia, A. Esrafil, R.R. Kalantary, Visible-light-driven photocatalytic degradation of Metalaxyl by reduced graphene oxide/Fe<sub>3</sub>O<sub>4</sub>/ZnO ternary nanohybrid: influential factors, mechanism and toxicity bioassay, *J. Photochem. Photobiol., A*, 375 (2019) 280–292.
- [19] Z. Wang, M. Chen, J. Shu, Y. Li, One-step solvothermal synthesis of Fe<sub>3</sub>O<sub>4</sub>@Cu@Cu<sub>2</sub>O nanocomposite as magnetically recyclable mimetic peroxidase, *J. Alloys Compd.*, 682 (2016) 432–440.
- [20] V.L. Pham, D.-G. Kim, S.-O. Ko, Cu@Fe<sub>3</sub>O<sub>4</sub> core-shell nanoparticle-catalyzed oxidative degradation of the antibiotic oxytetracycline in pre-treated landfill leachate, *Chemosphere*, 191 (2018) 639–650.
- [21] A. Fakhri, S. Rashidi, I. Tyagi, S. Agarwal, V.K. Gupta, Photodegradation of erythromycin antibiotic by γ-Fe<sub>2</sub>O<sub>3</sub>/SiO<sub>2</sub> nanocomposite: response surface methodology modeling and optimization, *J. Mol. Liq.*, 214 (2016) 378–383.
- [22] M. Hazarika, I. Saikia, J. Das, C. Tamuly, M.R. Das, Biosynthesis of Fe<sub>2</sub>O<sub>3</sub>@SiO<sub>2</sub> nanoparticles and its photocatalytic activity, *Mater. Lett.*, 164 (2016) 480–483.
- [23] A. Mohagheghian, K. Ayagh, K. Godini, M. Shirzad-Siboni, Enhanced photocatalytic activity of Fe<sub>3</sub>O<sub>4</sub>-WO<sub>3</sub>-APTES for azo dye removal from aqueous solutions in the presence of visible irradiation, *Part. Sci. Technol.*, 37 (2019) 358–370.
- [24] G. Zhao, Z. Mo, P. Zhang, B. Wang, X. Zhu, R. Guo, Synthesis of graphene/Fe<sub>3</sub>O<sub>4</sub>/NiO magnetic nanocomposites and its application in photocatalytic degradation of the organic pollutants in wastewater, *J. Porous Mater.*, 22 (2015) 1245–1253.
- [25] S. Wu, H. Hu, Y. Lin, J. Zhang, Y.H. Hu, Visible light photocatalytic degradation of tetracycline over TiO<sub>2</sub>, *Chem. Eng. J.*, 382 (2020) 122842, doi: 10.1016/j.cej.2019.122842.

- [26] L. Chen, C. Zhao, D.D. Dionysiou, K.E. O'Shea, TiO<sub>2</sub> photocatalytic degradation and detoxification of cylindrospermopsin, *J. Photochem. Photobiol., A*, 307 (2015) 115–122.
- [27] M. Khodadadi, T.J. Al-Musawi, H. Kamani, M.F. Silva, A. Hossein Panahi, The practical utility of the synthesis FeNi<sub>3</sub>@SiO<sub>2</sub>/TiO<sub>2</sub> magnetic nanoparticles as an efficient photocatalyst for the humic acid degradation, *Chemosphere*, 239 (2020) 124723, doi: 10.1016/j.chemosphere.2019.124723.
- [28] E. Bazrafshan, T.J. Al-Musawi, M.F. Silva, A. Hossein Panahi, M. Havangi, F.K. Mostafapur, Photocatalytic degradation of catechol using ZnO nanoparticles as catalyst: optimizing the experimental parameters using the Box–Behnken statistical methodology and kinetic studies, *Microchem. J.*, 147 (2019) 643–653.
- [29] N. Nasseh, A. Hossein Panahi, M. Esmati, N. Daglioglu, A. Asadi, H. Rajati, F. Khodadoost, Enhanced photocatalytic degradation of tetracycline from aqueous solution by a novel magnetically separable FeNi<sub>3</sub>/SiO<sub>2</sub>/ZnO nanocomposite under simulated sunlight: efficiency, stability, and kinetic studies, *J. Mol. Liq.*, 301 (2020) 112434, doi: 10.1016/j.molliq.2019.112434.
- [30] Z.B. Yu, Y.P. Xie, G. Liu, G.Q.M. Lu, X.L. Ma, H.-M. Cheng, Self-assembled CdS/Au/ZnO heterostructure induced by surface polar charges for efficient photocatalytic hydrogen evolution, *J. Mater. Chem. A*, 1 (2013) 2773–2776.
- [31] B. Li, Y. Wang, Facile synthesis and enhanced photocatalytic performance of flower-like ZnO hierarchical microstructures, *J. Phys. Chem. C*, 114 (2010) 890–896.
- [32] S. Balachandran, N. Prakash, K. Thirumalai, M. Muruganandham, M. Sillanpää, M. Swaminathan, Facile construction of heterostructured BiVO<sub>4</sub>–ZnO and its dual application of greater solar photocatalytic activity and self-cleaning property, *Ind. Eng. Chem. Res.*, 53 (2014) 8346–8356.
- [33] S. Banerjee, D.D. Dionysiou, S.C. Pillai, Self-cleaning applications of TiO<sub>2</sub> by photo-induced hydrophilicity and photocatalysis, *Appl. Catal., B*, 176 (2015) 396–428.
- [34] J. Yang, J. Wang, X. Li, D. Wang, H. Song, Synthesis of urchin-like Fe<sub>3</sub>O<sub>4</sub>@SiO<sub>2</sub>/ZnO/CdS core-shell microspheres for the repeated photocatalytic degradation of rhodamine B under visible light, *Catal. Sci. Technol.*, 6 (2016) 4525–4534.
- [35] N. Nasseh, T.J. Al-Musawi, M.R. Miri, S. Rodriguez-Couto, A. Hossein Panahi, A comprehensive study on the application of FeNi<sub>3</sub>@SiO<sub>2</sub>@ZnO magnetic nanocomposites as a novel photo-catalyst for degradation of tamoxifen in the presence of simulated sunlight, *Environ. Pollut.*, 261 (2020) 114127, doi: 10.1016/j.envpol.2020.114127.
- [36] A. Ajmal, I. Majeed, R.N. Malik, M. Iqbal, M.A. Nadeem, I. Hussain, S. Yousaf, G. Mustafa, M. Zafar, M.A. Nadeem, Photocatalytic degradation of textile dyes on Cu<sub>2</sub>O-CuO/TiO<sub>2</sub> anatase powders, *J. Environ. Chem. Eng.*, 4 (2016) 2138–2146.
- [37] S. Chabri, A. Dhara, B. Show, D. Adak, A. Sinha, N. Mukherjee, Mesoporous CuO–ZnO p–n heterojunction based nanocomposites with high specific surface area for enhanced photocatalysis and electrochemical sensing, *Catal. Sci. Technol.*, 6 (2016) 3238–3252.
- [38] A. Maleki, F. Moradi, B. Shahmoradi, R. Rezaee, S.-M. Lee, The photocatalytic removal of diazinon from aqueous solutions using tungsten oxide doped zinc oxide nanoparticles immobilized on glass substrate, *J. Mol. Liq.*, 297 (2020) 111918, doi: 10.1016/j.molliq.2019.111918.
- [39] C.S. Rajan, Nanotechnology in groundwater remediation, *Int. J. Environ. Sci. Dev.*, 2 (2011) 182–187.
- [40] J. Gao, B. Liu, J. Wang, X. Jin, R. Jiang, L. Liu, B. Wang, Y. Xu, Spectroscopic investigation on assisted sonocatalytic damage of bovine serum albumin (BSA) by metronidazole (MTZ) under ultrasonic irradiation combined with nano-sized ZnO, *Spectrochim. Acta, Part A*, 77 (2010) 895–901.
- [41] N. Nasseh, F.S. Arghavan, S. Rodriguez-Couto, A. Hossein Panahi, Synthesis of FeNi<sub>3</sub>/SiO<sub>2</sub>/CuS magnetic nano-composite as a novel adsorbent for Congo Red dye removal, *Int. J. Environ. Anal. Chem.*, (2020) 1–21, doi: 10.1080/03067319.2020.1754810.
- [42] H. Sun, B. Dong, G. Su, R. Gao, W. Liu, L. Song, L. Cao, Modification of TiO<sub>2</sub> nanotubes by WO<sub>3</sub> species for improving their photocatalytic activity, *Appl. Surf. Sci.*, 343 (2015) 181–187.
- [43] A. Falah-Shojaei, A. Shams-Nateri, M. Ghomashpasand, Synthesis and characterization of C-TiO<sub>2</sub>@Fe<sub>3</sub>O<sub>4</sub> magnetic nanoparticles for degradation Direct Blue 71 under visible light irradiation, *J. Color Sci. Technol.*, 4 (2014) 339–346.
- [44] A. Jahantiq, R. Ghanbari, A. Hossein Panahi, S.D. Ashraf, A.D. Khatibi, Photocatalytic degradation of 2,4,6-trichlorophenol in aqueous solutions using synthesized Fe-doped TiO<sub>2</sub> nanoparticles via response surface methodology, *Desal. Water Treat.*, 183 (2020) 366–373.
- [45] Y. Zandsalimi, A. Maleki, B. Shahmoradi, S. Dehestani, R. Rezaee, G. McKay, Photocatalytic removal of 2,4-dichlorophenoxyacetic acid from aqueous solution using tungsten oxide doped zinc oxide nanoparticles immobilized on glass beads, *Environ. Technol.*, (2020) 1–36, doi: 10.1080/09593330.2020.1797901.
- [46] Y. Abdollahi, A. Abdullah, Z. Zainal, N.A. Yusof, Synthesis and characterization of manganese doped ZnO nanoparticles, *Int. J. Basic Appl. Sci. (Dubai)*, 11 (2011) 62–69.
- [47] S. Vajapara, S. Patel, C.P. Bhasin, Efficient adsorption and photocatalytic degradation of Malachite Green dye using bentonite natural adsorbent, *Int. J. Nano. Chem.*, 3 (2017) 33–37.
- [48] A. Akyol, M. Bayramoğlu, Photocatalytic degradation of Remazol Red F3B using ZnO catalyst, *J. Hazard. Mater.*, 124 (2005) 241–246.
- [49] M. Khodadadi, M. Samadi, A. Rahmani, R. Maleki, A. Allahresani, R. Shahidi, Determination of organophosphorous and carbamate pesticides residue in drinking water resources of Hamadan in 2007, *Iran. J. Health Environ.*, 2 (2010) 250–257.
- [50] W. Leng, W. Zhu, J. Ni, Z. Zhang, J. Zhang, C.N. Cao, Photoelectrocatalytic destruction of organics using TiO<sub>2</sub> as photoanode with simultaneous production of H<sub>2</sub>O<sub>2</sub> at the cathode, *Appl. Catal., A*, 300 (2006) 24–35.
- [51] H. Lachheb, E. Puzenat, A. Houas, M. Ksibi, E. Elaloui, C. Guillard, J.-M. Herrmann, Photocatalytic degradation of various types of dyes (Alizarin S, Crocein Orange G, Methyl Red, Congo Red, Methylene Blue) in water by UV-irradiated titania, *Appl. Catal., B*, 39 (2002) 75–90.
- [52] H. Gao, T. Kan, S. Zhao, Y. Qian, X. Cheng, W. Wu, X. Wang, L. Zheng, Removal of anionic azo dyes from aqueous solution by functional ionic liquid cross-linked polymer, *J. Hazard. Mater.*, 261 (2013) 83–90.
- [53] Z. Noorimotlagh, G. Shams, H. Godini, R. Darvishi, Study of ZnO nano particles photocatalytic process efficiency in decolorization of methylene blue and COD removal from synthetic wastewater, *Yafteh*, 14 (2013) 51–61.
- [54] E. Norabadi, A. Hossein Panahi, R. Ghanbari, A. Meshkinian, H. Kamani, S.D. Ashrafi, Optimizing the parameters of amoxicillin removal in a photocatalysis/ozonation process using Box–Behnken response surface methodology, *Desal. Water Treat.*, 192 (2020) 234–240.
- [55] S. Chakrabarti, B.K. Dutta, Photocatalytic degradation of model textile dyes in wastewater using ZnO as semiconductor catalyst, *J. Hazard. Mater.*, 112 (2004) 269–278.
- [56] D.J. Naghan, A. Azari, N. Mirzaei, A. Velayati, F.A. Tapouk, S. Adabi, M. Pirsaeheb, K. Sharafi, Parameters effecting on photocatalytic degradation of the phenol from aqueous solutions in the presence of ZnO nanocatalyst under irradiation of UV-C light, *Bulg. Chem. Commun.*, 47 (2015) 14–18.
- [57] E. Dehghanifard, A.J. Jafari, R.R. Kalantari, M. Gholami, A. Esrafil, Photocatalytic removal of aniline from synthetic wastewater using ZnO nanoparticle under ultraviolet irradiation, *Iran. J. Health Environ.*, 5 (2012) 167–178.
- [58] Z. Guo, R. Ma, G. Li, Degradation of phenol by nanomaterial TiO<sub>2</sub> in wastewater, *Chem. Eng. J.*, 119 (2006) 55–59.
- [59] K. Salehi, R. Rahmani, B. Mansouri, N. Azadi, H. Ghafouri, U. Hamesadeghi, Performance evaluation of Ba:TiO<sub>2</sub> nanocomposite in photocatalytic degradation of Direct blue 71 in presence of sunlight, *Zanko J. Med. Sci.*, 18 (2017) 70–80.
- [60] F.S. Arghavan, T.J. Al-Musawi, E. Allahyari, M.H. Moslehi, N. Nasseh, A. Hossein Panahi, Complete degradation of tamoxifen using FeNi<sub>3</sub>@SiO<sub>2</sub>@ZnO as a photocatalyst with

- UV light irradiation: a study on the degradation process and sensitivity analysis using ANN tool, *Mater. Sci. Semicond. Process.*, 128 (2021) 105725, doi: 10.1016/j.mssp.2021.105725.
- [61] F.S. Arghavan, A. Hossein Panahi, N. Nasseh, M. Ghadirian, Adsorption-photocatalytic processes for removal of pentachlorophenol contaminant using FeNi<sub>3</sub>/SiO<sub>2</sub>/ZnO magnetic nanocomposite under simulated solar light irradiation, *Environ. Sci. Pollut. Res.*, 28 (2021) 7462–7475.
- [62] B. Shahmoradi, I. Ibrahim, K. Namratha, N. Sakamoto, S. Ananda, R. Somashekar, K. Byrappa, Surface modification of indium doped ZnO hybrid nanoparticles with n-butylamine, *Int. J. Chem. Eng. Res.*, 2 (2010) 107–117.
- [63] H. Chen, H. Luo, Y. Lan, T. Dong, B. Hu, Y. Wang, Removal of tetracycline from aqueous solutions using polyvinylpyrrolidone (PVP-K30) modified nanoscale zero valent iron, *J. Hazard. Mater.*, 192 (2011) 44–53.
- [64] M. Gar Alalm, A. Tawfik, S. Ookawara, W. Treatment, Solar photocatalytic degradation of phenol by TiO<sub>2</sub>/AC prepared by temperature impregnation method, *Desal. Water Treat.*, 57 (2016) 835–844.